

Nomenclature

C	mushy zone constant, $\text{kg/m}^3\text{s}$
C_p	specific heat, J/kg K
g	gravitational acceleration, m^2/s
h	sensible enthalpy, J/kg
H	enthalpy, J/kg
k	thermal conductivity, W/mK
L	latent heat fusion, J/kg
T	temperature, K
u	velocity, m/s

Greek symbols

μ	dynamic viscosity of the fluid, Kg/ms
ρ	density, kg/m^3
ν	kinematics viscosity, m/s^2
β	liquid fraction

and solar collectors. Khodadadi and Zhang [25] studied the effect of buoyancy-driven convection on constrained melting of PCM in a spherical container numerically. Their results showed the rate of melting at the top region of sphere is faster than at the bottom region due to increase conduction.

Assis et al. [26] investigated both numerically and experimentally on melting in a spherical shell. They performed their numerical studies using the commercial software Fluent 6.0. Computational results had a good agreement with experimental results for different wall temperatures and different shell diameters. They presented a correlation for the melting fraction based on the Grashof, Stefan and Fourier numbers. They performed another combined experimental and numerical study on the solidification of PCM inside a spherical shell with various diameters [27]. Tan and Leong [28] carried out an experimental study of solidification of pure n-Octadecane within two rectangular cells with different aspect ratios and three different constant heat fluxes. Their results showed that a faster rate of solidification occurred at higher heat rates and smaller aspect ratios. Hosseiniadeh et al. [29] investigated both experimental and numerical study of constrained and unconstrained melting in a spherical container using n-Octadecane as PCM that was initially subcooled to 1°C .

Alawadhi [30] carried out a numerical study on transient laminar flow past an in-line cylinders array containing phase change material (PCM) using the finite-element method. He investigated a parametric study of heat exchanges between the PCM and flow at different Reynolds numbers and pitch to diameter ratios whereas Prandtl number was fixed at 0.71. His predicted results show that the Reynolds number has a significant effect on the PCM melting time, whereas the pitch to diameter ratio has an insignificant effect.

Bagheri et al. [31] studied the transient behaviour of a thermal storage module numerically. The module is composed of a concentric tube, in which the annulus contains the phase-change material (PCM) and the inner tube carries the heat transfer fluid. They used three different PCM. They measured the charging time for every PCM at the same condition. Hosseiniadeh et al. [32] studied the unconstrained melting of nano-enhanced phase change materials (NEPCM) inside a spherical container using RT27 and copper particles as base material and nano-particle, respectively. They found that the enhancement in the thermal conductivity and decrease of latent heat increase the melting rate of NEPCM compared to conventional PCM.

Ng et al. [33] carried out a numerical simulation of convection melting of a PCM in a cylindrical annulus heated isothermally from the inside wall. The impacts of Rayleigh number on the melting rate as well as the evolution of the fluid flow pattern were investigated. It was found that enhancements in Rayleigh number increase heat transfer rate. Also, melting of PCM in the bottom section was very ineffective because the energy modified to the system was mostly transferred to the upper section. Liu et al. [34] studied experimentally the solidification of stearic acid in a vertical annulus energy storage system. They used a copper fin mounted to the electrical heating source to promote the thermal conductivity of the base material. It was concluded that the rate of heat transfer was directly associated with the inlet temperature and the Reynolds number had just a very slight effect on the solidification rate. Melting process of a pure PCM in tube geometries of two various configurations (square external tube with a circular tube inside and circular external tube with a square tube inside) were investigated numerically by Khillarkar et al. [35]. It was observed that the thermal stratification obtained in the upper section of the cavity because of the natural convection. Mesalhy et al. [36] performed a numerical study for increasing the thermal conductivity of PCM using porous matrix in two concentric cylinders. They found that the presence of porous matrix had an influential effect on the melting rate of PCM while it damped the convection motion. In this way, the decreases of the porosity enhanced the melting rate.

This paper presents numerical study of melting between two cylinders for concentric and eccentric state. This study was done to investigate the effect of position of inner cylindrical tube on melting of PCM (charging) in outer cylindrical shell. It can be important in shell and tube heat exchangers problem.

2. Governing equations

In the numerical study, the flow is considered unsteady, laminar, incompressible and two-dimensional. The viscous dissipation term is considered negligible. The viscous incompressible flow and the temperature distribution are solved using the Navier–Stokes and thermal energy equations, respectively. Consequently, the continuity, momentum, and thermal energy equations can be expressed as follows:

Continuity:

$$\partial_t(\rho) + \partial_i(\rho u_i) = 0. \quad (1)$$

Momentum:

$$\partial_t(\rho u_i) + \partial_j(\rho u_i u_j) = \mu \partial_{jj} u_i - \partial_i p + \rho g_i + S_i. \quad (2)$$

Thermal energy:

$$\partial_t(\rho h) + \partial_t(\rho \Delta H) + \partial_i(\rho u_i h) = \partial_i(k \partial_i T). \quad (3)$$

In these relations, u_i is the fluid velocity, ρ is the PCM's density, μ is the dynamics viscosity, P is the pressure, g is the gravitational acceleration, k is the thermal conductivity and h is the sensible enthalpy which is defined as follows:

$$h = h_{ref} + \int_{T_{ref}}^T C_p dT. \quad (4)$$

The enthalpy, H , is therefore:

$$H = h + \Delta H. \quad (5)$$

ΔH is the latent heat content that may vary between zero (solid) and L (liquid), the latent heat of the PCM. Therefore, liquid fraction β , can be defined as follows:

$$\beta = \begin{cases} \frac{\Delta H}{L} = 0 & \text{if } T < T_{solidus}, \\ \frac{\Delta H}{L} = 1 & \text{if } T > T_{liquidus}, \\ \frac{\Delta H}{L} = \frac{T - T_{solidus}}{T_{liquidus} - T_{solidus}} & \text{if } T_{solidus} < T < T_{liquidus}. \end{cases} \quad (6)$$

In Eq. (2), S_i is the Darcy's law damping terms (as source term) that are added to the momentum equation due to phase change effect on convection. It is defined as follows:

$$S_i = \frac{C(1 - \beta)^2}{\beta^3} u_i. \quad (7)$$

The coefficient C is a mushy zone constant which is fixed at a value of $10^5 \text{ kg/m}^3\text{s}$ for the present study [37].

3. Numerical procedures

Numerical study of the present problem is solved using the commercial software FLUENT 6.3.26. The computational domain of the symmetric model is shown in Fig. 1. The small cylinder's inner diameter and wall thickness are 20 and

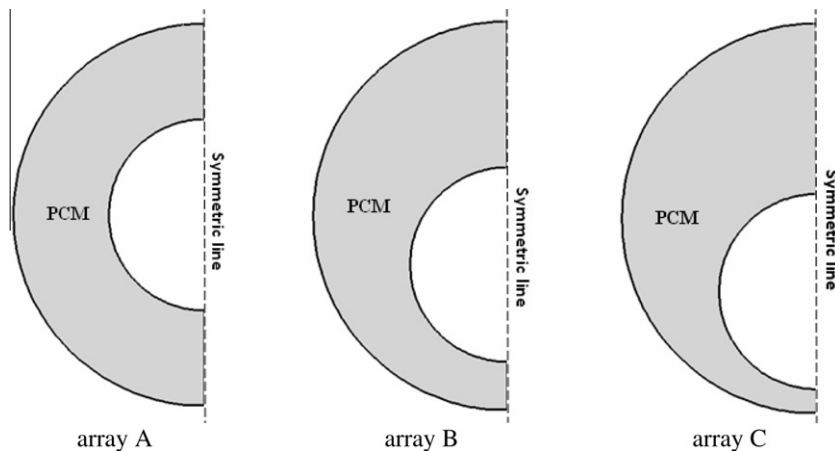


Fig. 1. Schematic of computational domain.

Table 1
Thermophysical properties of N-eicosane.

Properties	Values
Melting temperature	36 (35–37) °C
Density	770 kg/m ³
Kinematic viscosity	5×10^{-6} m ² /s
Specific heat	2460 J/kg K
Thermal conductivity	0.1505 W/m K
Latent heat of fusion	247.6 kJ/kg
Thermal expansion coefficient	0.0009 K ⁻¹

1.5 mm, respectively. The outer cylinder's diameter is 40 mm. and the thermal conductivity of inner cylinder is equal to 400 (W/m K). The cylinders are concentric in array A, and the centre-to-centre distances are 5 and 7.5 mm in array B and C, respectively. N-eicosane is selected as PCM that its thermophysical properties are taken in Table 1. The inner cylinder tube is hot and outer cylinder tube is insulated. PCM is sub-cooled to 1 °C.

In order to solve the momentum and energy equations, the power law differencing scheme and the SIMPLE method for pressure–velocity coupling are used. Also the PRESTO scheme is adopted for the pressure correction equation. The under-relaxation factors for the velocity components, pressure correction, thermal energy and liquid fraction are 0.2, 0.3, 1 and 0.9, respectively. Different grid sizes were selected and tested to ensure independency of solution from the adopted grid size based on comparison of melting fraction and streamline contours. An arrangement of 6470 grids was found sufficient for the present numerical study. Adoption of fine grid distribution in the radial direction allows the use of longer time steps. The time duration to achieve full melting is a good indicator of time step dependence. The PCM melted after 47.4, 58.7 and 61.2 min with time step increments of 0.01, 0.005 and 0.002 s for concentric position (array A), respectively. Therefore, the time step is set 0.005 s. The number of iterations for every time step fixed at 70 was found sufficient to satisfy the convergence criteria (10^{-5}). In order to validate the present work, initial run is done and compared with work of Assis et al. [26] for temperature difference of 10 °C ($Ste = 0.1$) and shell diameter of 40 (mm). Fig. 2 shows comparison of liquid fraction versus time between two works. It can be seen that the present study shows a good agreement with Assis et al. [26] work.

4. Results and discussion

Instantaneous colorized contours of solid-liquid front at different time (after 1, 5, 10, 15 and 20 min) are presented for three different arrays of cylinders in Fig. 3. The solid PCM was subcooled at 308.15 °C where the wall temperature of inner cylinder fixed to the 329.15 °C.

It can be seen, at start, very thin layer of liquid is formed around hot inner cylinder symmetrically for all arrays. After 5 min, this layer is expanded. Although the shape and size of liquid zones are approximately the same in each three arrays, solid PCM is more melted in top region of inner cylinder. It is due to the effect of natural convection in this zone where warm liquid rises to the top region and cooler liquid replaces. Heat conduction occurs between hot surface of inner wall and cold solid PCM at the bottom region. This phenomenon is shown schematically in Fig. 4. Also the predicted result shows an

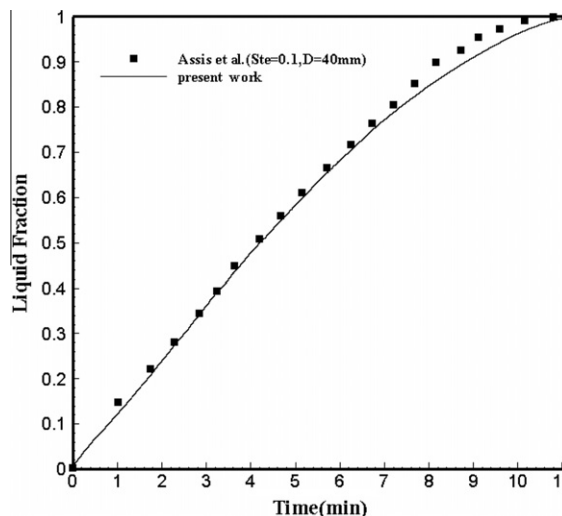


Fig. 2. Comparison of liquid fraction versus time between present study and Assis et al. [26] work.

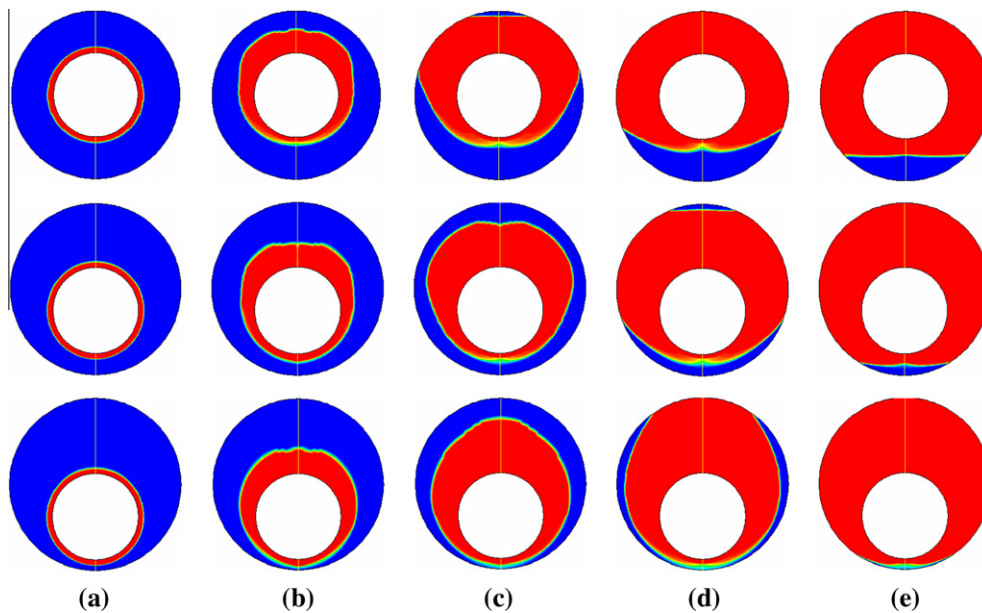


Fig. 3. Computational melting phase front for different arrays with sub-cooling of 1 °C (blue colour: solid PCM). (For interpretation of the references to colour in this figure legend, the reader is referred to the web version of this article.)

unstable and complicated structure near the top region of the cylinder that brings about the formation of waviness on the solid–liquid interface.

As time progresses further, the shape of liquid zones is different from each other. After 10 min, liquid layer reaches to the outer cylinder in array A while it can be seen a thick layer of solid PCM near this wall in two others. It is due to less distance of hot cylinder to top section of outer cylinder. This phenomenon occurs for array B after 15 min while exist a layer of solid near bottom and sides of outer cylinder for array C.

After 20 min, all of solid PCM is approximately melted in array C whereas significant quantity of it remained in bottom region in array A. So the long-time needs to complete melting.

Streamlines and isotherms at various time instants for each array are shown in Fig. 5.

Streamlines in left half section of symmetric line are drawn with black lines whereas colorized isotherm lines are drawn in right half of it. It is observed that the several recirculation regions create in the narrow melting area which shows the Benard formation in natural convection (Fig. 5(b and c)). It should be mention that by increasing the melting area, several recirculation regions merge to gather and create a main recirculation region (Fig. 5(e)). The temperature distribution in the melting area is affected by recirculation formation. This phenomenon can be seen in the Fig. 5 clearly. Although the melting zone (mass of liquid divided to total mass) in array C is larger than B and A (Fig. 3(e)), the overall temperature in this area for array C is lower than for two others.

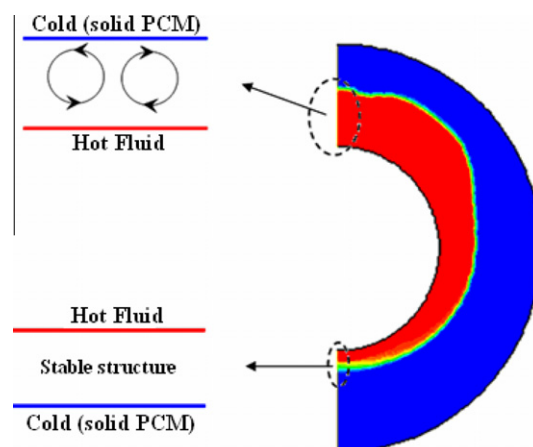


Fig. 4. Stable and unstable structures of thermal layers in symmetric line.

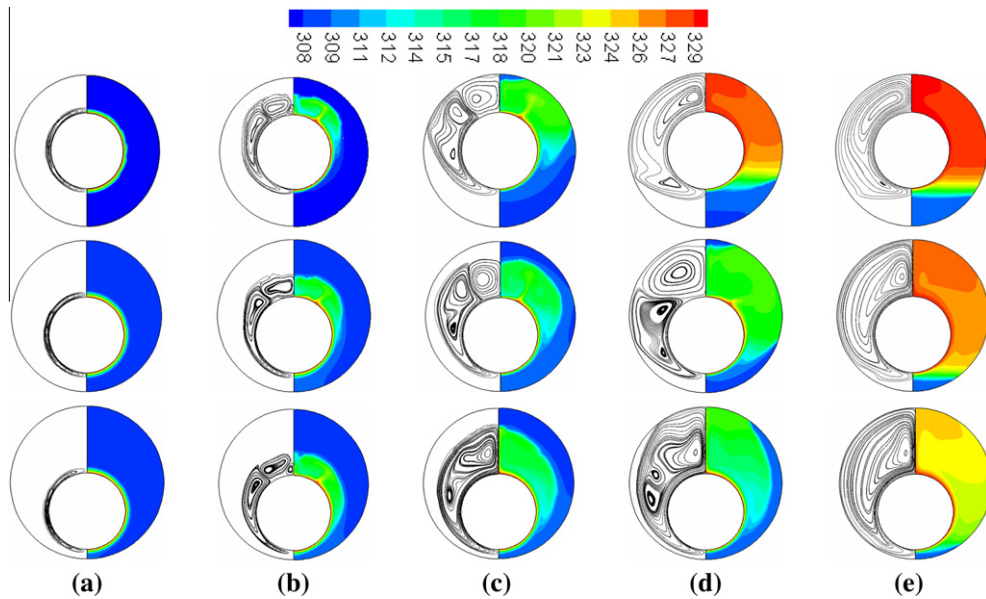


Fig. 5. Streamlines and isotherms for different arrays at various times.

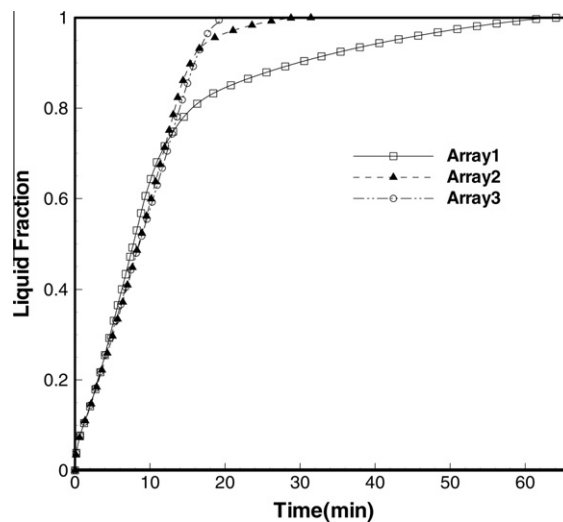


Fig. 6. Variation of liquid fraction versus time.

Liquid fraction versus times is plotted in Fig. 6. It reveals that the curves have linear behaviours for all arrays before 15 min approximately. In these times, the volume of melted PCM in array A is slightly greater than other arrays. After 15 min, curve for array C continued linear variation while both others turn in curvature lines for other arrays especially for array A. As discussed above, in this time, Solid PCM melted in top region of cylinders and therefore, pure heat conduction is dominated mechanism of heat transfer between solid PCM and inner cylinders for array A and B. On the other hand, in array C, a layer of solid PCM exists around inner sides of outer cylinder yet. Thus combined heat conduction and natural heat convection cause to continue linear change of melting rate in this array. Full melting for array A, B and C occur 58.7, 26.08 and 20.2 min, respectively. It is interesting when inner cylinder tube staggered 5 mm (as same as inner tube radius) toward down of centre, the melting rate increases to twice approximately.

5. Conclusion

In present study, the melting of PCM was investigated in concentric and eccentric cylindrical tubes. The PCM sub-cooled to 1 °C. Predicted results show that heat conduction to the PCM is dominant at the beginning of melting for all zones through

contact melting. After a few minutes, natural convection becomes dominant at top half of hot cylinder while heat conduction remains dominant in bottom of hot cylinder. Thus melting rate in top half becomes faster than the bottom half of the cylinder. It is interesting when inner cylinder tube moves toward down of the centre, the melting rate increases sharply. It is due to dominant the natural convection heat transfer in the most area of PCM.

References

- [1] G.A. Lane, *Solar Heat Storage: Latent Heat Material*, vol. II, Technology, CRC Press, Florida, 1986.
- [2] M. Kamimoto, Y. Abe, S. Sawata, T. Tani, T. Ozawa, Latent heat storage unit using form-stable high density polyethylene for solar thermal applications, in: *Proceedings of the International Symposium on Thermal Application of Solar Energy*, Hakone (Kanagawa, Japan), 1985.
- [3] M. Hadjieva, S. Kanev, J. Argirov, Thermo physical properties of some paraffins applicable to thermal energy storage, *Sol. Energ. Mater.* 27 (1992) 181–187.
- [4] V.H. Morcos, Investigation of a latent heat thermal energy storage system, *Sol. Wind. Technol.* 7 (2/3) (1990) 197–202.
- [5] L.F. Cabeza, J. Roca, M. Nogues, B. Zalba, J.M. Marin, Transportation and conservation of temperature sensitive materials with phase change materials: state of the art, IEA ECES IA Annex 17 2nd Workshop, Ljubljana, Slovenia, 2002.
- [6] M.A. Cuevas-Diarte, T. Calvet-Pallas, J.L. Tamarit, H.A.J. Oonk, D. Mondieig, Y. Haget, Nuevos materiales termoajustables, *MundoCientífico*, June 2000.
- [7] D. Pal, Y. Joshi, Application of phase change materials for passive thermal control of plastic quad flat packages: a computational study, *Numer. Heat Tran. A* 30 (1996) 19–34.
- [8] M. Koschenz, B. Lehmann, Development of a thermally activated ceiling panel with PCM for application in lightweight and retrofitted buildings, *Energ. Build.* 36 (2002) 567–578.
- [9] J.K. Kisson, J.M. Hannig, T.I. Whitney, M.L. Drake, Testing and simulation of phase change wallboard for thermal storage in buildings, in: *Proceedings of 1998 International Solar Energy Conference*, pp. 45–52, New York, USA, 1998.
- [10] J. Bellettre, V. Sartre, F. Biais, A. Lallemand, Transient state study of electric motor heating and phase change solid–liquid cooling, *Appl. Therm. Eng.* 17 (1) (1997) 17–31.
- [11] L.L. Vasiliev, V.S. Burak, A.G. Kulakov, D.A. Mishkinis, P.V. Bohan, Latent heat storage modules for preheating internal combustion engines: application to a bus petrol engine, *Appl. Therm. Eng.* 20 (2000) 913–923.
- [12] M. Telkes, E. Raymond, Storing solar heat in chemicals – a report on the Dover house, *Heat Vent.* 46 (11) (1949) 80–86.
- [13] H.G. Barkmann, F.C. Wessling, Use of buildings structural components for thermal storage, in: *Proceedings of the Workshop on Solar Energy Storage Subsystems for the Heating and Cooling of Buildings*, Charlottesville (Virginia), USA, 1975.
- [14] D.W. Hawes, D. Feldman, D. Banu, Latent heat storage in building materials, *Energ. Build.* 20 (1993) 77–86.
- [15] Y. Morikawa, H. Suzuki, F. Okagawa, K. Kanki, A development of building elements using PCM, in: *Proceedings of the International Symposium on Thermal Application of Solar Energy*, Hakone (Kanagawa), Japan, 1985.
- [16] C.H. Lee, H.K. Choi, Crystalline morphology in high-density polyethylene/paraffin blend for thermal energy storage, *Polym. Compos.* 19 (6) (1998) 704–708.
- [17] M. Sokolov, Y. Keizman, Performance indicators for solar pipes with phase change storage, *Sol. Energ.* 47 (1991) 339–346.
- [18] Y. Rabin, I. Bar-Niv, E. Korin, B. Mikic, Integrated solar collector storage system based on a salt-hydrate phase change material, *Sol. Energ.* 55 (1995) 435–444.
- [19] S.O. Enibe, Performance of a natural circulation air heating system with phase change material energy storage, *Renew. Energ.* 27 (2002) 69–86.
- [20] S.O. Enibe, Parametric effects on the performance of a passive solar air heater with storage, in: *Proceedings of the World Renewable Energy Congress VII*, Cologne, Germany, 2002.
- [21] J. Tey, R. Fernandez, J. Rosell, M. Ibanez, Solar collector with integrated storage and Transparent insulation cover, in: *Proceedings of Eurosun*, Bologna, Italy, 2002.
- [22] F. Agyenim, N. Hewitt, P. Eames, M. Smyth, A review of materials, heat transfer and phase change problem formulation for latent heat thermal energy storage systems (LHTES), *Renew. Sust. Energ. Rev.* 14 (2010) 615–628.
- [23] M.M. Farid, A.M. Khudhair, S.A.K. Razack, S. Al-Hallaj, A review on phase change energy storage: materials and applications, *Energ. Convers. Manage.* 45 (2004) 1597–1615.
- [24] B. Zalba, J.M. Marin, L.F. Cabeza, H. Mehling, Review on thermal energy storage with phase change: materials, heat transfer analysis and applications, *Appl. Therm. Eng.* 23 (2003) 251–283.
- [25] J.M. Khodadadi, Y. Zhang, Effects of buoyancy-driven convection on melting within spherical containers, *Int. J. Heat Mass Tran.* 44 (2001) 1605–1618.
- [26] E. Assis, L. Katsman, G. Ziskind, R. Letan, Numerical and experimental study of melting in a spherical shell, *Int. J. Heat Mass Tran.* 50 (2007) 790–1804.
- [27] E. Assis, G. Ziskind, R. Letan, Numerical and experimental study of solidification in a spherical shell, *J. Heat Trans.* 31 (1) (2009) 24502–24507.
- [28] F.L. Tan, K.C. Leong, Conjugate solidification inside a thick mold, *J. Mater. Process. Technol.* 89–90 (1999) 159–164.
- [29] S. F. Hosseiniadeh, F. L. Tan, J. M. Khodadadi, A.A. Rabienataj Darzi, Experimental and Numerical Investigation of Unconstrained Melting inside a Spherical Container, in: *Seventh International Conference on Heat Transfer, Fluid Mechanics and Thermodynamic*, pp. 1999–2004, Antalya, Turkey, 2010.
- [30] E.M. Alawadhi, Thermal analysis of transient laminar flow past an in-line cylinders array containing phase change material, *Proc. IMechE A J. Power Energ.* 223 (4) (2009) 349–360.
- [31] G.H. Bagheri, M.A. Mehrabian, K. Hooman, Numerical study of the transient behaviour of a thermal storage module containing phase-change material, *Proc. IMechE A J. Power Energ.* 224 (4) (2010) 349–360.
- [32] S.F. Hosseiniadeh, A.A. Rabienataj Darzi, F.L. Tan, Numerical investigations of unconstrained melting of nano-enhanced phase change material (NEPCM) inside a spherical container, *Int. J. Therm. Sci.* 51 (2012) 77–83.
- [33] K.W. Ng, Z.X. Gong, A.S. Mujumdar, Heat transfer in free convection-dominated melting of phase change material in horizontal annulus, *Int. Comm. Heat Mass Tran.* 25 (5) (1998) 631–640.
- [34] Z. Liu, X. Sun, C. Ma, Experimental study of the characteristics of solidification of stearic acid in an annulus and its thermal conductivity enhancement, *Energ. Convers. Manage.* 46 (2005) 971–984.
- [35] D.B. Khillarkar, Z.X. Gong, A.S. Mujumdar, Melting of a phase change material in concentric horizontal annuli of arbitrary cross-section, *Appl. Therm. Eng.* 20 (2000) 893–912.
- [36] O. Mesalhy, K. Lafdi, A. Elgafy, K. Bowman, Numerical study for enhancing the thermal conductivity of the phase change material (PCM) storage using high thermal conductivity porous matrix, *Energ. Convers. Manage.* 46 (2005) 847–867.
- [37] A.D. Brent, V.R. Voller, K.J. Reid, Enthalpy-porosity technique for modeling convection-diffusion phase change: application to the melting of a pure metal, *Numer. Heat Tran.* 13 (1988) 297–318.